A SCALABLE ELECTRONIC SENSOR FOR MULTIPLEXED DETECTION OF CELLS IN DIFFERENT MICROFLUIDIC CHANNELS

*R. Liu, N. Wang, W. Waheed, and A. F. Sarioglu**
Georgia Institute of Technology, Atlanta, Georgia, USA

ABSTRACT

Microfluidic devices are extremely attractive for performing a wide variety of biomedical assays, some of which rely on accurate determination of spatial information from manipulated particles/biological cells. To obtain this spatial information, microfluidic devices are often tied to microscopic analysis leading to complex instrumentation with higher cost and reduced portability. To address these shortcomings, we introduce a sensor technology, microfluidic CODES, that combines resistive pulse sensing with code division multiple access (CDMA) to detect the particles/cells in multiple channels from a single electrical waveform. We designed and fabricated a proof-of-principle microfluidic device and characterized it by processing a simulated biological sample of human cancer cells. By post-processing, we decoded the electrical signal and successfully identified cells in different microfluidic channels, even if cell signals overlap. Microfluidic CODES has the potential to enable low-cost integrated lab-on-a-chip devices that are ideally suited for point-of-care testing of clinical samples.

INTRODUCTION

Analysis of micro-sized particles such as cells, bacteria or viruses using lab-on-a-chip devices continues to be a major area of research that is poised to revolutionize point-of-care testing of biological samples. Numerous biological assays can be performed by spatially tracking particles on lab-on-a-chip devices, where cells/functionalized particles are sorted or captured based on their biophysical [1] or biochemical [2] properties. In most devices, such spatial information is only available through microscopic analysis, limiting the practical utility of the microfluidic chip by tying it to a lab infrastructure, and also increasing the complexity of a system-level implementation. Therefore, an on-chip sensor that can spatially track manipulated particles on a microfluidic chip can potentially enable low-cost, integrated lab-on-a-chip devices that are particularly attractive for testing of biological samples in resource-limited settings.

Among various sensing modalities, resistive pulse sensing (RPS) [3] offers a simple and robust method for label-free detection of small particles and forms the basis of commercially available Coulter counters, widely used for micro-particle sizing and counting. Specifically, RPS relies on modulation of the impedance between two electrodes as a particle, suspended in an electrolyte, passes through an aperture that is placed between two electrodes. By incorporating miniaturized electrodes in microfluidic channels, microscale resistive pulse sensors were successfully used to detect particles ranging from blood cells to viruses [4-5]. With the goal of increasing the device throughput, devices with multiple microfluidic channels equipped with dedicated resistive pulse sensors have previously been demonstrated [6-8]. However, these devices are more complex as they require interfacing with a large number of electrodes and have limited scalability.

In this paper, we introduce a simple and scalable technology, named Microfluidic Coded Orthogonal Detection by Electrical Sensing (microfluidic CODES), to create a multiplexed network of resistive pulse sensors that can be used to spatially track particles on microfluidic devices. We achieve multiplexing by designing micromachined sensors such that each generates distinct electrical waveforms when a particle is detected. We specifically design orthogonal signal waveforms similar to the digital codes used in code division multiple access (CDMA) telecommunication networks, so that individual sensor signals can be uniquely recovered from a single output waveform, even if signals from different sensors interfere. Therefore, our approach allows us to achieve multiplexing of resistive pulse sensors without increasing the number of external electrode connections to the microfluidic device, keeping both device- and system-level complexity to a minimum. We created a microfluidic device with four channels as a proof of the concept. Using human ovarian cancer cells in phosphate-buffered saline (PBS) as a model biological system, we demonstrated that individual cells in different microfluidic channels could be uniquely identified.

DIGITAL CODE DESIGN

To design an orthogonal digital code set, we used the mathematical principles of CDMA telecommunication networks [9]. CDMA is a spread spectrum communication technique, where multiple users simultaneously communicate with a base station through a shared communication channel. Multiplexing of information in CDMA is accomplished by modulating individual user signals with assigned distinct digital codes, called digital spreading codes. By using a decoder that is matched to a specific user's digital spreading code, the information from any user can be retrieved with minimal effect from interference from other users. In this way, CDMA allows multiplexed transmission of information simultaneously and within the same frequency band.

A set of distinguishable codes is a critical requirement for a successful implementation of a CDMA system. Ideally, the digital code set should be perfectly orthogonal, i.e., cross-correlation between different digital codes is zero. While it is possible to design a perfectly orthogonal code set for synchronously transmitted signals, only quasi-orthogonal signal sets with bounded cross-correlation properties can be designed for asynchronous CDMA systems. Randomly arriving cells in microfluidic channels constitutes an asynchronous system and therefore a code-set that maintains its orthogonality under random phase shifts is required. To address these requirements, we used Gold sequences [10] that have both desirable autocorrelation and cross-correlation properties and therefore are commonly employed in asynchronous CDMA uplink to minimize multi-user interference.

To encode four microfluidic channels, we designed 7-bit long Gold sequences. In this process, we first generated a pair of 7-bit long preferred maximal length pseudorandom noise sequences (*m*-sequences). To achieve this, we created two linear feedback shift-registers (LFSRs) based on two primitive polynomials: x^3+x^2+1 and x^3+x+1. We initialized the two LFSRs at 001 and 111 states, respectively and obtained a preferred pair of *m*-sequences: m_1=1001011 and m_2=1110100. We then added cyclic shifts of m_1 and m_2 using bitwise XOR operation to obtain a set of nine 7-bit long Gold sequences. We also tested the validity of the generated sequences by analyzing their autocorrelation and cross-correlation properties. Finally, we chose four 7-bit Gold sequences (g_1=1010110, g_2=0111111, g_3=0100010, g_4=0011000) as digital codes to encode four microfluidic channels.

MICROFLUIDIC CHIP DESIGN & FABRICATION

To demonstrate microfluidic CODES technology, we designed and fabricated a four-channel microfluidic device (Figure 1(a)). RPS signal waveforms can be created by micromachining the electrodes [11-12] or the microfluidic channels [13]. In our device, we micropatterned three coplanar electrodes to form a network of electrode fingers at the bottom of each microfluidic channel. Each electrode finger is 10 μm wide and is separated from the neighboring electrode finger by a 10 μm gap. We designed the electrode finger pitch to be on the order of a typical cell size and this leads to localized modulation of impedance between electrode finger pairs as cells flow through microfluidic channels. This way, we use the sequential interaction of the flowing particles with the electrode finger array to generate distinct orthogonal digital codes in different microfluidic channels.

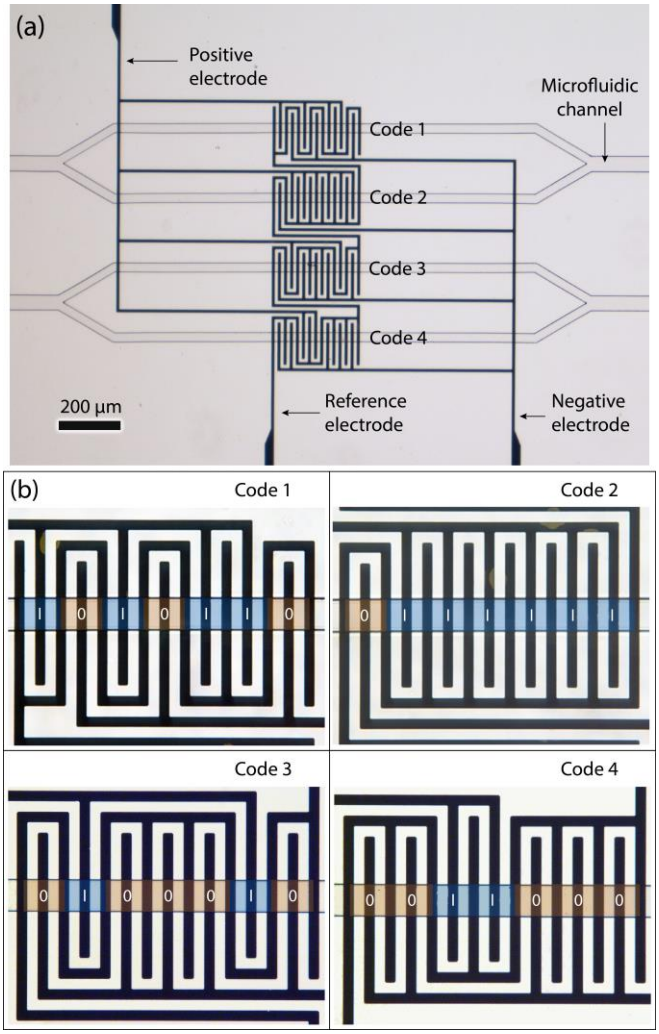

Figure 1. Image of the microfluidic CODES device (a) Full image of the four channel device composed coding surface electrodes on a glass substrate and PDMS microfluidic channels (b) A close-up image of coding electrodes producing 7-bit Gold sequences: "1010110", "0111111", "0100010", "0011000".

An important advantage of our electrode network design is its ability to produce bipolar RPS signals. Bipolar signals are less prone to interference than unipolar signals as they lead to lower cross-correlation between different codes. To generate bipolar signals, our electrode design includes a third electrode as a reference since the impedance modulation between a pair of electrodes is inherently unipolar. Using differential impedance modulation in this configuration allows us to directly generate digital codes in a bipolar form similar to the codes generated using Binary Phase Shift Keying (BPSK) modulation in wireless CDMA communication networks.

We developed a systematic approach to micropattern three electrodes to create a sensor network that can generate any digital code in an arbitrary number of microfluidic channels (Figure 1(a)). First, positive and negative electrodes are placed at the opposite sides of each microfluidic channel. Then we extend these electrodes to form electrode fingers crossing microfluidic channels. The order of positive and negative fingers along each microfluidic channel is determined based on the digital code uniquely assigned for each channel. Second, we route the reference electrode between each pair of positive and negative electrodes fingers. In this configuration, the center-to-center distance between two consecutive reference electrode fingers constitutes a single bit of the digital code. The type of the electrode finger (positive or negative) between two reference electrode fingers determines the polarity (1 or 0) of each bit. Finally, we place the positive and negative electrode traces far from the outer reference electrodes in order to minimize the conduction outside of the coding region.

Another important aspect of our electrode design is that it forms a balanced impedance network to maximize device sensitivity. To achieve this, we first design a code set that contains an equal total number of "1"s and "0"s. This enables us to use an equal number of positive and negative electrode fingers in our layout. When configured as such, the static impedances between the reference and positive/negative electrodes are balanced. This improves the sensitivity of the device since the dynamic impedance changes due to particles are not dominated by the suppressed background signal due to static impedance difference. In addition, the balanced sensor signal is more robust, i.e., less affected by the fluid or material properties.

To fabricate our device, we used a combination of surface micromachining and soft lithography. The device consists of a glass substrate with surface electrodes and a polydimethylsiloxane (PDMS) microfluidic layer. The surface electrodes were fabricated using a lift-off process. Briefly, a 1.5 μm-thick negative photoresist film on a 4-inch glass wafer was patterned using photolithography. A 100 nm-thick Cr/Au film stack was deposited using e-beam evaporation and underlying photoresist was etched in acetone under sonication. The microfluidic channel layer was fabricated using soft lithography. A 15 μm-thick SU-8 photoresist was spun on a silicon wafer and then patterned using photolithography to create the mold. The mold was subsequently coated with a 10:1 mixture of PDMS prepolymer and cross-linker. Degassed PDMS polymer was cured at 65 °C for 4 hours and cured PDMS is peeled off from the mold. PDMS layer and diced glass chips were surface activated under oxygen plasma and were bonded to form the final device (Figure 1).

EXPERIMENTAL METHODS

To characterize our device, we used cells suspended in PBS as a model biological sample. We cultured HeyA8 ovarian cancer cell line (obtained from Dr. John F. McDonald, Georgia Institute of Technology) in RPMI 1640 media (Cellgro, Herndon, VA) supplemented with 10% fetal bovine serum (FBS; Seradigm, Radnor, PA) and 1% penicillin (aMResco, Solon, OH) under a 5% CO_2 atmosphere at 37 °C until a 80% confluence is reached. Following a short trypsinization step, cells were pelleted and then suspended in PBS solution.

In our experiment, suspended cells were driven through the microfluidic device at a constant flow rate using a syringe pump.

The electrical signal from the device was acquired using a data acquisition system. The cell transit was also recorded using a microscope equipped with a high-speed camera to verify the validity of the sensor signals. The complete experimental system is shown in Figure 2.

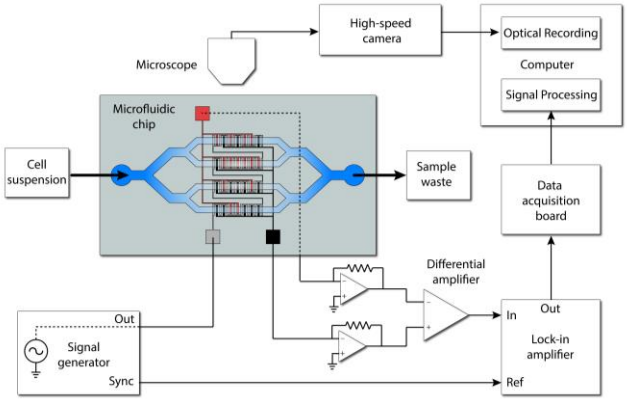

Figure 2. The Experimental setup used for our measurements: cell suspension is driven through the microfluidic chip using a syringe pump. A bipolar electrical signal is generated using a differential amplifier and is sampled into a computer for decoding. High-speed optical microscopy is used to validate decoded electrical signals

We measured changes in the current flow between the surface electrodes as the cells pass through the microfluidic channels. Specifically, we applied a 400 kHz AC signal to the reference electrode and measured the current flow from negative and positive electrodes separately using two transimpedance amplifiers. We then obtained the differential impedance signal by subtracting the positive electrode signal from the negative electrode signal using a differential amplifier. The amplitude of the resulting bipolar signal was measured using a lock-in amplifier, and the lock-in amplifier output was sampled into the computer at 1 MHz through a data acquisition board for post-processing. During these measurements, the microfluidic chip was placed on an inverted optical microscope (Nikon Eclipse Ti-E) and imaged using a high-speed camera (Vision Research Phantom v7.3). A video of cells flowing through the microfluidic device was recorded at a rate of 8000 frames per second. Recorded videos were downloaded into a computer and compared with the simultaneously recorded electrical signals from our sensor. Frame by frame analysis of the microscopy images enabled us to test the accuracy of our results.

RESULTS AND DISSCUSSION

Distinct digital codes from each microfluidic channel can clearly be identified in the recorded sensor signal. The sensor signals match well with the designed Gold sequences (Figure 3(a)). Deviations are due to several factors such as non-uniform current flow between coplanar electrodes, spherical cell geometry and the coupling between electrodes in the network.

We processed the signal using MATLAB to analyze and decode individual digital spreading codes as follows: for each cell, we first measure the time between signal peaks to determine the bit duration, which we use to generate a template library of four square pulse sequences (each corresponding to a microfluidic channel). Correlating the signal with these four square pulse sequences, we obtain a dominant autocorrelation peak uniquely identifying the microfluidic channel the cell passed through (Figure 3(b)).

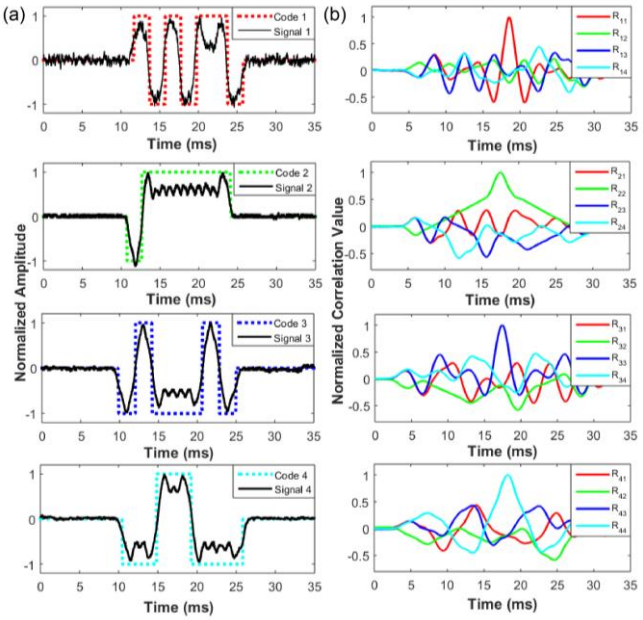

Figure 3. Decoding the electrical signal. (a) Normalized sensor signals corresponding to each microfluidic channel are shown with corresponding ideal square pulse sequences. (b) Each signal is correlated with the set of four square pulse code sequences and is decoded through an autocorrelation peak.

It should also be noted that unlike a CDMA communication network in which digital pulses are generated electronically, temporal properties of our digital spreading codes are determined by the microfluidic flow speed. In order to minimize variations in flow speed between different microfluidic channels, we designed all four microfluidic channels to have equal hydraulic resistances. We also choose the microfluidic channel cross section to be close to the cell size so that cell speed is less affected by the non-uniform flow profile across the channel.

An important feature of our technology is that it can resolve cells in microfluidic channels even when they overlap in time. This is quite important for processing samples with high density of particles, where overlapping cases are more frequently to occur. When multiple cells occupy the coding region simultaneously, the interference between signals makes it hard to identify individual cells (Figure 4(a)). Here, we demonstrate a case where we resolve two overlapping cells (Figure 4). We first estimate the bit duration for both cells using the signal peaks in the non-overlapping region. Following our decoding scheme explained before, we determined from two autocorrelation peaks that the cells were in the third and fourth microfluidic channels (Figure 4(b)). This was also confirmed from the simultaneously recorded images by high-speed optical microscopy (Figure 4(c)). In addition, this approach is also valid to identify cells overlapping within the same microfluidic channel, since it can be considered as interference of the same digital spreading code with its own time-shifted version.

In addition to detecting the presence of cells in microfluidic channels, our technology can also resolve their timing. This is because our digital codes are very sensitive to time-shifts and produce sharp autocorrelation peaks only at zero time delay. For example, we measured the time delay between the two cells in Figure 4 to be ~1.9 ms from the autocorrelation peaks. The same time delay was estimated to be ~2.1 ms from the simultaneously recorded video, validating our result.

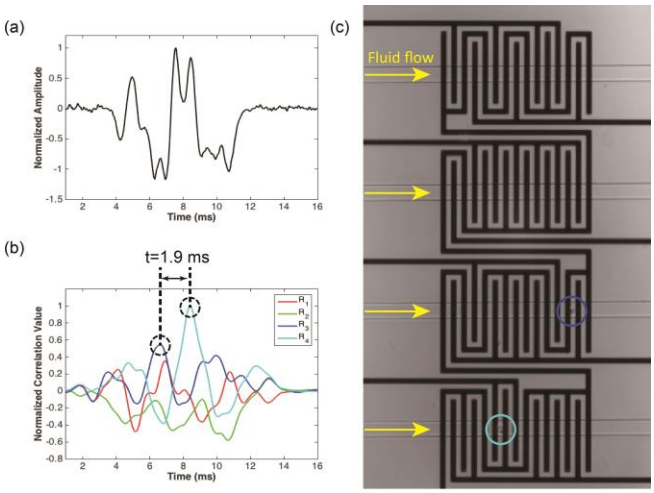

Figure 4. Decoding of the overlapping signals. (a) Two cells occupy the coding region at the same time and sensor signals with each other. (b) Correlation calculations determine which channels cells were in and also the amount of time delay between them from autocorrelation peaks. (c) Simultaneously recorded images using high-speed optical microscopy validate results.

Finally, the peak amplitudes in autocorrelation plots should be interpreted carefully as they are affected by several factors including the size of the cell, the proximity of the cell to surface electrodes and interference in the case of overlapping events. First, larger cells lead to larger signals and therefore higher autocorrelation peaks. For example, optical image in Figure 4 shows that the cell in the fourth microfluidic channel is slightly larger and is also associated with the larger autocorrelation peak. Second, the closer the cell is to the surface electrodes, the larger the signal and hence the autocorrelation peak is. To minimize the variations due to this effect and also to utilize it in increasing the sensitivity, we designed our microfluidic channel to be 15 µm-high. Third, the peak autocorrelation value is affected by the cross-correlation properties of digital spreading codes when cells overlap. While the use of orthogonal digital codes such as Gold sequences minimizes this effect, peak autocorrelation value might still change due to constructive or destructive interference.

CONCLUSION

Combining the techniques from telecommunications and microfluidics, we have introduced a scalable electronic sensor technology, microfluidic CODES, to detect particles in multiple microfluidic channels from a single electrical output. Microfluidic CODES incorporates a multiplexed network of resistive pulse sensors into a microfluidic chip such that each sensor produces a distinct digital code when a particle is detected. These digital codes were designed using the principles of coding in CDMA telecommunication networks and could be uniquely recovered through simple mathematical calculations even when they interfere. We also demonstrated that our technology could readily be applied to detect human ovarian cancer cells on a multi-channel microfluidic chip. Microfluidic CODES offers a simple, all-electronic interface to spatially track particles on microfluidic devices, which will potentially be useful in creating integrated low-cost lab-on-a-chip assays.

ACKNOWLEDGEMENTS

This work was supported by the start-up funds for Dr. A. F. Sarioglu, by Georgia Institute of Technology, School of Electrical and Computer Engineering. The authors would like to thank Chia-Heng Chu for his help in preparation of the manuscript.

REFERENCES

[1] A. F. Sarioglu, N. Aceto, N. Kojic, M. C. Donaldson, M. Zeinali, B. Hamza, A. Engstrom, H. Zhu, T. K. Sundaresan, D. T. Miyamoto, X. Luo, A. Bardia, B. S. Wittner, S. Ramaswamy, T. Shioda, D. T. Ting, S. L. Stott, R. Kapur, S. Maheswaran, D. A. Haber, and M. Toner, "A microfluidic device for label-free, physical capture of circulating tumor cell clusters", Nature Methods, 12, 685, (2015).

[2] S. Nagrath, L. V. Sequist, S. Maheswaran, D. W. Bell, D. Irimia, L. Ulkus, M. R. Smith, E. L. Kwak, S. Digumarthy, A. Muzikansky, P. Ryan, U. J. Balis, R. G. Tompkins, D. A. Haber, and M. Toner, "Isolation of rare circulating tumour cells in cancer patients by microchip technology", Nature, 450, 1235, (2007).

[3] R. W. DeBlois and C. P. Bean, "Counting and sizing of submicron particles by the resistive pulse technique", Review of Scientific Instruments, 41, 909, (1970).

[4] S. Gawad, L. Schild, and P. Renaud, "Micromachined impedance spectroscopy flow cytometer for cell analysis and particle sizing", Lab on a Chip, 1, 76, (2001).

[5] N. N. Watkins, S. Sridhar, X. Cheng, G. D. Chen, M. Toner, W. Rodriguez, and R. Bashir, "A microfabricated electrical differential counter for the selective enumeration of CD4+ T lymphocytes", Lab on a Chip, 11, 1437, (2011).

[6] J. Zhe, A. Jagtiani, P. Dutta, J. Hu, and J. Carletta, "A micromachined high throughput Coulter counter for bioparticle detection and counting", Journal of Micromechanics and Microengineering, 17, 304, (2007).

[7] Y. Song, J. Yangi, X. Pan, and D. Li, "High-throughput and sensitive particle counting by a novel microfluidic differential resistive pulse sensor with multidetecting channels and a common reference channel", Electrophoresis, 36, 495, (2015).

[8] A. V. Jagtiani, J. Carletta, and J. Zhe, "A microfluidic multichannel resistive pulse sensor using frequency division multiplexing for high throughput counting of micro particles", Journal of Micromechanics and Microengineering, 21, 065004 (2011).

[9] D. Torrieri, Principles of Spread-Spectrum Communication Systems, Springer, New York, 2015.

[10] R. Gold, "Optimal binary sequences for spread spectrum multiplexing", IEEE Transactions on Information Theory, 13, 619, (1967).

[11] D. Polling, S. C. Deane, M. R. Burcher, C. Glasse, and C. H. Reccius, "Coded electrodes for low signal-noise ratio single cell detection in flow-through impedance spectroscopy", Proceedings of uTAS, Groningen, The Netherlands, October 3–7, (2010),.

[12] S. Emaminejad, S. Talebi, R. W. Davis, and M. Javanmard, "Multielectrode Sensing for Extraction of Signal From Noise in Impedance Cytometry", IEEE Sensors Journal, 15, 2715, (2015).

[13] K. R. Balakrishnan, G. Anwar, M. R. Chapman, T. Nguyen, A. Kesavaraju, and L. L. Sohn, "Node-pore sensing: a robust, high-dynamic range method for detecting biological species", Lab on a Chip, 13, 1302, (2013).

CONTACT

*A. F. Sarioglu, tel: +1-404-894-5032; sarioglu@gatech.edu